Dalton Transactions

Accepted Manuscript

ROYAL SOCIETY OF CHEMISTRY

www.rsc.org/dalton

Dalton Transactions

RSCPublishing

COMMUNICATION

Ion coordination significantly enhancing photocatalytic activity of graphitic-phase carbon nitride

Cite this: DOI: 10.1039/x0xx00000x

Received ooth January 2012,
Accepted ooth January 2012

DOI: 10.1039/x0xx00000x

www.rsc.org/dalton

Honglin Gao,[a, b] Shicheng Yan,[a] Jiajia Wang,[a] and Zhigang Zou[a, c]

Here we report a facile surface modification route, metal ion coordination, to improve the photoactivity of carbon nitride. The metal ions coordinating into the plane of g-C_3N_4 significantly contributes to a drastic increase of the photocatalytic activity in solar hydrogen production as well as in photodegradation of organic pollutant.

Photocatalysis is considered as a potentially available technique for solar hydrogen production as well as organic contaminants decomposition.[1] To use this technique, an efficient photocatalytic material is needed. The ideal photocatalytic material would combine an ability to dissociate the water molecules, having a band gap that absorbs light in the visible range and be efficient in separating, collecting and transporting charges for the chemical processes.[2, 3] Besides, it should be non-toxic, abundant and low-cost for large-scale applications.[4] The graphitic carbon nitride (g-C_3N_4) is an optimal photocatalytic material to satisfy the most of requirement, and has been used to split water[5] and degrade organic pollutants[6]. However, photocatalytic activity of the g-C_3N_4 is unsatisfactory for a purpose of practical applications, probably owing to the inefficient carrier separation and transport. Several routes, such as forming organic-inorganic heterojunctions[7] and constructing high-conductivity composite[8], have been explored for improving the efficiency in separation and transportation of charges. In these routes, the enhancement in separation of carriers is not outstanding due to the limited contact area between bulk materials. The separation and transportation of charge carriers in the C_3N_4 sheet, which usually are the rate-limiting step for photocatalytic reaction, are expected to further improve for constructing the efficient g-C_3N_4-based photocatalytic reaction system.

For the photocatalytic reaction to occur, the photogenerated carriers should be transferred to the surface of the photocatalyst, and then reacted with the adsorbed species. Therefore, surface modification affected the photocatalytic activity for a given photocatalyst. Some surface modification routes, such as adsorption of ionic species, defects and doping, were found to be the useful methods to improve the performance of photocatalysts such as TiO_2 and $SrTiO_3$[9, 10]. Here, we found that the photocatalytic activity of g-C_3N_4 can be easily improved by a facile ion coordination route. After dispersing the g-C_3N_4 powders into the metal ions-containing salt solution, the g-C_3N_4 exhibits the strong ability in capture of cation by ion-dipole interaction between the cations and the negatively charged nitrogen atoms of g-C_3N_4. The ion coordination route improves the separation and transfer of charge carriers, thus significantly enhancing the photocatalytic activity of g-C_3N_4. Such a route is not only effective for solar hydrogen production, but also useful for degradation of pollutants.

The g-C_3N_4 photocatalyst used in this study was prepared by heating melamine at 500 ^oC for 2h and 520 ^oC for another 2h, as described in our previous report.[6] The crystal structure of g-C_3N_4 is confirmed by XRD (see Fig. S1), which belongs to a layered solid with ABA stacking of graphene-like C-N sheet. A large nitrogen pots in plane of g-C_3N_4 is composed of 3-fold N-bridge linking the triazine units (Fig. 1a), where are filled with six nitrogen lone-pair electrons. It is well-known that a C-O ring in 18-crown-6 exhibits the strong ability to capture metal cations such as K^+ and Na^+ by forming ion-dipole interaction between the cations and the negatively charged oxygen atoms of the polyether ring.[11] Compared to the charged oxygen atoms of C-O ring of 18-crown-6, the nitrogen atoms of nitrogen pots of g-C_3N_4 also are potentially ideal sites for metal ions inclusion with stronger coordination ability due to the more lone-pair electrons. Therefore, it offers a chance to improve the photoactivity of g-C_3N_4 by ion coordination route. As an initial trial to improve photoactivity of g-C_3N_4 by ion coordination route, the photocatalytic hydrogen production experiments were carried out by dispersing the g-C_3N_4 powders into simulated seawater with main components including NaCl, $MgCl_2$, Na_2SO_4 and KCl (see Table S1) under visible light irradiation. Using 10 vol. % tri-ethanolamine as an electron donor and 0.5wt% Pt as a cocatalyst, as shown in Fig.1b that the hydrogen production rate from simulated seawater reaches to 0.399 mmol g^{-1} h^{-1}, is 5.5 times higher than 0.072 mmol g^{-1} h^{-1}, as measured from deionized water. The enhanced hydrogen production would originate from the effect of ions existed in seawater on the photocatalytic activity of g-C_3N_4. To confirm this fact, the H_2 production over g-C_3N_4 was estimated under the addition of individual NaCl, Na_2SO_4, KCl, K_2SO_4 or $MgCl_2$ into the deionized

water. The results indicate that all of the ions used in this study can improve the hydrogen production over g-C_3N_4 (Fig. 1b, see Table 1).

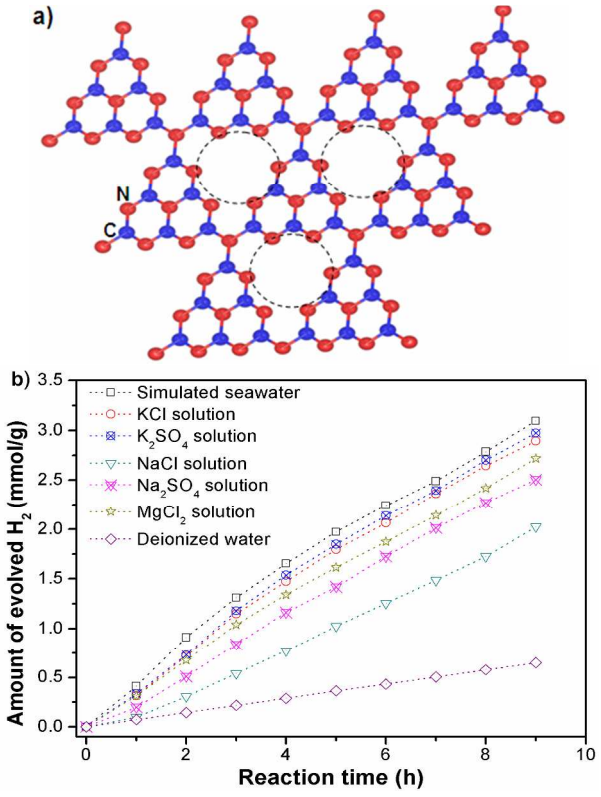

Figure 1. (a) Schematic diagram of a perfect graphitic carbon nitride sheet constructed from tri-s-triazine units. ○ indicates the nitrogen pots which filled with six nitrogen lone-pair electrons potentially ideal sites for metal inclusion. (b) Hydrogen production from the simulated seawater and the various salt solutions. Catalyst: 0.1 g-C_3N_4; Light irradiation: wavelength larger than 420 nm; 10 vol. % triethanolamine as an electron donor and 0.5wt% Pt as a cocatalyst.

Table 1. Fluorescence lifetimes (FL), apparent quantum yield (AQY), non-radiative rate (NR), electrical conductivity (EC), hydrogen evolution rate (HER) and BET surface area for g-C_3N_4 and C_3N_4-salt samples

Samples	FL (ns)	AQY (%)	NR k_{nr} (ns^{-1})	EC $\times10^{-7}$ (Scm^{-1})	HER (μmol g^{-1} h^{-1})
g-C_3N_4	4.99	9.7	0.18	0.108	72
C_3N_4-KCl	0.037	7.2	25.08	0.198	332
C_3N_4-$MgCl_2$	2.86	7.2	0.32	0.120	299
C_3N_4-Na_2SO_4	4.30	8.1	0.21	0.109	287
C_3N_4-NaCl	4.56	8.4	0.20	0.111	229

The zeta potential is an efficient parameter to indicate the surface charge of materials, which can provide the evidence for the interaction between g-C_3N_4 and ions. In our case, the change in zeta potential for dispersing the g-C_3N_4 into diffrent ions obtaining aqueous solution exhibits the similar trend with increasing the ion concentration. Taking KCl for example (Fig. 2), the zeta potential of g-C_3N_4 without KCl is determined to be 25.4 mV. Upon the addition of KCl, it is obvious that the zeta potential of g-C_3N_4 decreases from 25.4 to 13.8 mV as concentration of potassium chloride (C_K) increases from 0 to 0.1 mM, followed by a more gradual decrease to 4.9 mV as the KCl concentration increases to 10 mM. The reduction of the zeta potential upon the addition of salt can be elaborated using the electric double layer theory which provides a quantitative understanding of the surface-charge development process for adsorption of aqueous ions onto the surface of the g-C_3N_4. [12] The cation, K^+, can coordinate into nitrogen pots of g-C_3N_4 surface (Fig. 1a), and the counter Cl^- anions enter the stern layer of g-C_3N_4 suspension particles. Thus, the zeta potential decreases with increase of KCl concentration. The electrical conductivity of the solution with the low KCl content keeps no change when the zeta potential decreases. This further indicates that the most of ions were coordinated into the surface of g-C_3N_4 particles when the low concentration of ions was added into the g-C_3N_4 suspension. The ion coordination into surface of g-C_3N_4 reaches to saturation when the concentration of KCl more than 10 mM, and the zeta potential of g-C_3N_4 particles and electrical conductivity of the solution increase with the increase of KCl concentration.

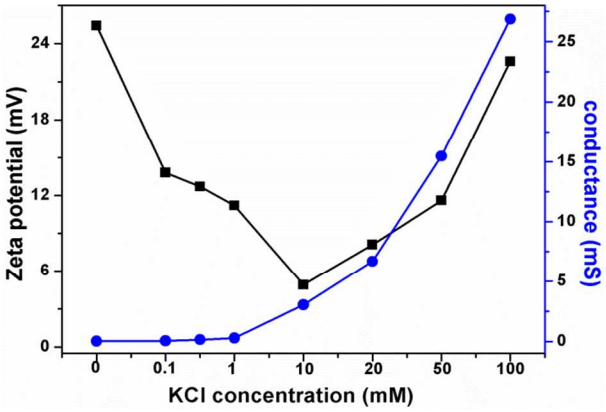

Figure 2. Zeta potential for the g-C_3N_4 particles in KCl solution and electrical conductivity of KCl containing g-C_3N_4 suspension.

To further understand the effect of the ions on photoactivity of g-C_3N_4, the g-C_3N_4 powders were respectively dispersed into the saturated salt solution for 2 h, dried at 80 °C and the obtained sample was denoted as C_3N_4-NaCl, C_3N_4-KCl, C_3N_4-$MgCl_2$, C_3N_4-K_2SO_4 and C_3N_4-Na_2SO_4. There are no changes in XRD patterns, UV-Vis absorbance spectra and TEM observations (see Fig. S1，S2 and S3) for g-C_3N_4 before and after salt soaking treatment, indicating that the salt soaking treatment does not change the bulk characteristic of g-C_3N_4. FTIR spectrum was used to probe the structure information of the g-C_3N_4 before and after salt soaking treatment, as shown in Fig. 3. For the g-C_3N_4 and C_3N_4-salt samples, several strong bands in the 1200-1650 cm^- region were found, which correspond to the typical stretching modes of CN heterocycles. Additionally, the characteristic breathing mode of the triazine units at 805 cm^- was observed. This indicated that the salt soaking treatment did not change the main structure of g-C_3N_4. It is obvious that two new peaks appeared at 708 and 793 cm^- for all samples after salt soaking treatment. The peak at 708 cm^- can be assigned to the out of plane bending mode of the C-N heterocycle, which exhibited a slight shift if compared to the 709 cm^- for the graphite-like domains with nitrogen atoms. The small shift probably resulted from the 3-fold N-bridge capturing the metal cation, as shown in Figure 1a. The peak at 793 cm^- is the indication of C-H bond.[14] The C-H bond formation further indicated that the metal cation coordinating into the nitrogen pots decreased the interaction between C and N atoms. It should be pointed out that the

intensity of peak at 708 cm^{-} for the C_3N_4-NaCl is slightly weaker than the C_3N_4-Na_2SO_4, implying that the anions affect the interaction between metal cation and nitrogen pots. For the sulfate soaking samples (C_3N_4-Na_2SO_4 and C_3N_4-K_2SO_4) , a new peak at 615cm^{-} was found, which is the indication of the SO_4^{2-} of sulfate,[15] meaning that the metal ions are stabilized in the electron-rich nitride pots of g-C_3N_4 through ion-dipole interaction, as well as by charge balance via ion interaction between anion and cation. The weak interaction between metal cation and nitrogen pots in C_3N_4-NaCl induced the low photocatalytic performance in hydrogen production if compared to C_3N_4-Na_2SO_4, as shown in Figure 1b. However, the hydrogen production rate in the K_2SO_4 solution is nearly the same as in KCl solution (Fig. 1b), indicating that there is a strong interaction between K^+ and nitrogen pots, that is, the effect of anion can be ignored when the K^+ was used as the ligand. This means that the K^+ coordination is a good choice for improving the photocatalytic activity of g-C_3N_4, as demonstrated in the hydrogen production.

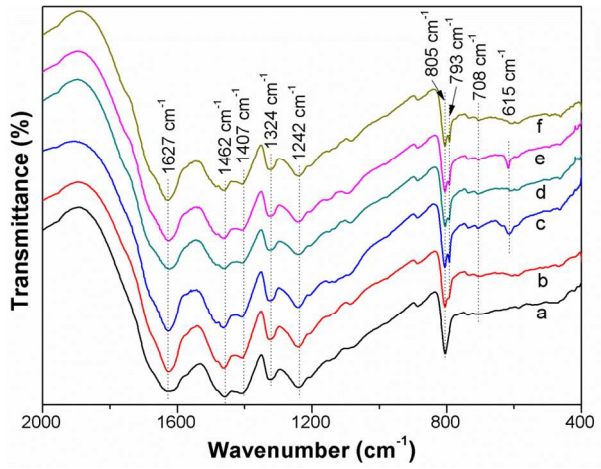

Figure 3 FT-IR spectra of g-C_3N_4 and C_3N_4-salt samples. (a) g-C_3N_4, (b) C_3N_4-NaCl, (c) C_3N_4-Na_2SO_4, (d) C_3N_4-KCl, (e) C_3N_4-K_2SO_4, (f) C_3N_4-$MgCl_2$

The ^{13}C and ^{15}N cross-polarization magic-angle spinning (CP-MAS) NMR spectra for g-C_3N_4 and C_3N_4-KCl were obtained for providing the information about effect of ion coordination on charge transfer. The ^{13}C spectra (Fig. 4a) signals of 165 ppm and 155.1 ppm are attributed to the formation of a poly(tri-s-triazine) structure characteristic of carbon nitride.[16, 17] After soaking treatment in KCl solution, the signals of ^{13}C obtained C_3N_4-KCl is changed into 163.8 ppm and 155.8 ppm, indicated that there is an interaction between ions and carbon nitrogen plane.[18] The ^{15}N CP-MAS spectra signals (Fig. 4b) of g-C_3N_4 can be assigned to the bridging NH groups (δ = -244 ppm), the outer ring nitrogen atoms of the heptazine or triazine rings (δ=-170 to -204 ppm), and the amino groups (δ=-260 to -280 ppm).[17,19] Compared to g-C_3N_4, the signals of ^{15}N NMR spectrum of C_3N_4-KCl exhibits the obvious change in chemical shift in δ = -170 to -204 ppm, revealing that cations can coordinate into heptazine or triazine rings of g-C_3N_4. The changes in chemical shift of ^{13}C and ^{15}N NMR spectra would indicate that after salt soaking treatment the electron transfer paths in g-C_3N_4 plane is changed. The new electron transfer paths improve the seperation and transport of photogenerated carriers, thus contributing to the enhancement of photoactivity of g-C_3N_4.

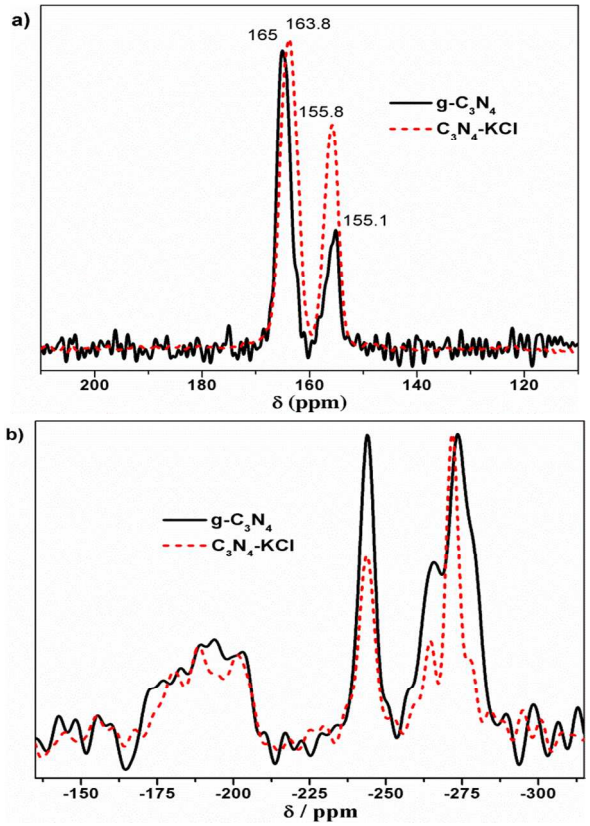

Figure 4. ^{13}C (a) and ^{15}N (b) CP-MAS solid-state NMR spectra of g-C_3N_4 and C_3N_4-KCl

To further confirm the formation of novel electron transfer paths in the g-C_3N_4 soaking treatment by salt, the fluorescence measurement was performed. The photoluminescence (PL) spectra for the g-C_3N_4 powders after soaking treatment in different salt solutions for 2h as compared with the sample without soaking are shown in Fig. 5a. The pure g-C_3N_4 showed the highest fluorescence intensity, which decreased upon additional ions. Since time-resolved fluorescence measurements provide more information than is available from the steady-state data and fluorescence lifetimes are typically independent of the probe concentration,[20] we measured the intensity decays of these samples by use of a single photon counting setup. Fluorescence lifetimes extracted from the decay curves are given in Table 1. In accordance with the steady-state PL spectra, the fluorescence lifetime decreased from 4.99 ns for the g-C_3N_4 down to 4.56-0.037 ns (Fig. 5b) for all of the samples treated by different salt solutions. This is due to an increased nonradiative rate (K_{nr}), that is, K_{nr} = 0.18 and 0.20-25.08 ns^{-1} for g-C_3N_4 and the g-C_3N_4 samples after soaking in different salt solutions (Table 1), respectively. The quenching of the emission intensity and its lifetime indicate that the relaxation of g-C_3N_4 excitations occurs via nonradiative paths,[3, 21] presumably by charge transfer of electrons and holes to new localized states which were formed by ion coordination. The new charge transfer paths can be an indication for the photoactivity of materials.

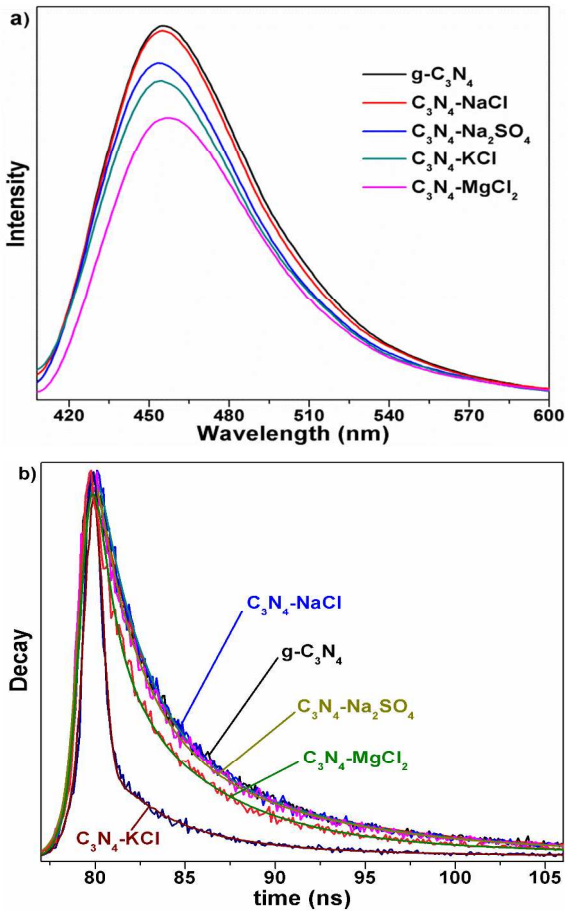

Figure 5. (a) Photoluminescence (PL) spectra for the g-C_3N_4 and the g-C_3N_4 after soaking treatment in different salt solutions. (b) Fluorescence decay of g-C_3N_4 before and after soaking treatment in different salt solutions with an excitation wavelength of 350 nm.

In addition, the bulk electrical conductivity, which usually depends on the carrier concentration and carrier mobility in semiconductors[22], was detected by a standard four-probe method. The electrical conductivity of all the ion-modified g-C_3N_4 (0.109-0.198×10^{-7} S cm^{-1}, depending on the ions) is higher than that of pure g-C_3N_4 (0.108×10^{-7} S cm^{-1}) (Table 1). Compared to g-C_3N_4, the C_3N_4-KCl and C_3N_4-$MgCl_2$ exhibit the obvious increase in conductivity, while for the C_3N_4-NaCl and C_3N_4-Na_2SO_4 the slight increase in conductivity is detected. The difference in conductivity probably implies that the ions of K and Mg have the stronger coordination ability than Na ion, and thus the higher photoactivity in solar hydrogen production. This means that the coordination of ions into g-C_3N_4 improves the conductivity, which facilitates the transfer of photogenerated carriers, thus enhancing the oxidation-reduction kinetics of water.

Advantage of such a simple route to enhance the photo-activity of g-C_3N_4 was also demonstrated in the removal of organic pollutants. Dispersing the g-C_3N_4 powders into the KCl or Na_2SO_4-containing methyl orange (MO) solution, a clear demonstration of the ion coordination induced g-C_3N_4 photocatalytic superiority is shown the evolution of MO degradation as a function of time under illumination at a wavelength larger than 420 nm (Fig. 6a). The g-C_3N_4 fully degraded the MO dye after 5h, while the photodegradation of MO can be achieved in 1.33 h and 0.75 h by adding Na_2SO_4 and KCl into the reaction system, respectively. After adding the ions into the MO solution, the adsorption amount of MO dye on the surface of g-C_3N_4 decreases slightly. Therefore, the enhanced photodegradation rate by ion adding would result from the ion coordination inducing high photoactivity of g-C_3N_4.

The kinetics of MO photodegradation on the g-C_3N_4 surface can be described by the first-order equation of $\ln(C_0/C)=k\cdot t$.[23] where C_0 is the initial concentration of MO, C is the actual concentration of MO at light irradiation time t, and k is the degradation rate constant (min^{-1}). Figure 6b present the linear relationship between $\ln(C_0/C)$ and the irradiation time. The k is determined from the slope of the line when $\ln(C_0/C)$ is plotted versus the corresponding irradiation time, thus the value of k gives an indication of the activity of the photocatalyst. Apparently, for the MO photodegradation, the ions-containing solutions exhibit the rate constant of 0.033 min^{-1} for Na_2SO_4 solution and 0.058 for KCl solution, which are respectively 3 and 5 times higher than the 0.011 min^{-1} for the deionized water. This evidence confirms that the rate constants of photodegrading MO are increased by adding of ions.

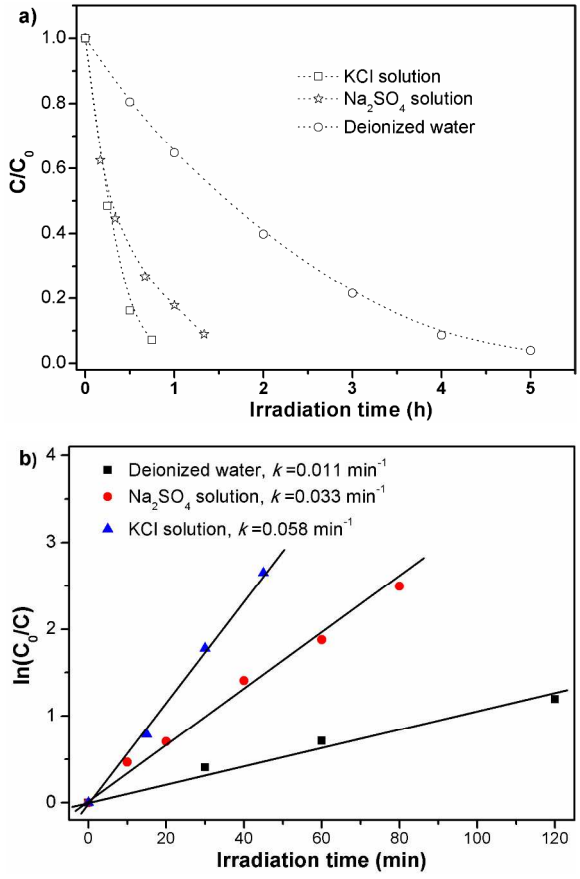

Figure 6. Photodegradation of methyl orange (a) and relationship between the degradation efficiency and the light irradiation time (b) over g-C_3N_4 under different ions-containing solutions. Catalyst: 0.3g; Light irradiation: wavelength larger than 420 nm.

Conclusions

In summary, the present studies have demonstrated that the photoactivity of carbon nitride can be efficiently improved by a simple ion coordination route. Introducing the ions to the plane of g-C_3N_4 is an efficient surface modification method to improve the

separation and transport of charge carriers useful for the enhancement of photocatalytic activities in solar hydrogen production as well as degradation of organic pollutants. Our results open up the new opportunities for using the cheap g-C_3N_4 material as an efficient photocatalyst applied in various fields. The facile and efficient surface modification method probably is applicable for improving the photoactivity of organic semiconduting photocatalyst in solar energy conversion into the chemical energy such as H_2 evolution and CO_2 photoreduction.

This work was supported by the National Basic Research Program of China (973 Program, 2013CB632404) and the National Natural Science Foundation of China (No. 51102132, 11174129, 51272101, and 51272102).

Notes and references

[a] Eco-Materials and Renewable Energy Research Center (ERERC), College of Engineering and Applied Sciences, Nanjing University, NO. 22, Hankou Road, Nanjing, Jiangsu 210093, P. R. China. Fax: 025-83686632; Tel: 025-83686639; E-mail: yscfei@nju.edu.cn; zgzou@nju.edu.cn

[b] Research Institute of Engineering and technology, Yunnan University, NO.2, North Cuihu road, kunming, Yunnan 650091, P.R. China

[c] National Laboratory of Solid State Microstructures, School of Physics, Nanjing University, NO. 22, Hankou Road, Nanjing, Jiangsu 210093, P. R. China

† Electronic Supplementary Information (ESI) available: Experimental procedures, characterization data, XRD, FT-IR spectra, and optical measurements. See DOI: 10.1039/c000000x/

1 H. Tong, S. X. Ouyang, Y. P. Bi, N. Umezawa, M. Oshikiri and J. H. Ye, *Adv. Mater.* 2012, **24**, 229-251.
2 Y. Tachibana, L. Vayssieres and J. R. Durrant, *Nat. Photon.* 2012, **6**, 511-518.
3 H. Kisch, *Angew. Chem. Int. Ed.* 2013, **52**, 812-847.
4 A. Kubacka, M. Fernánder-García and G. Colón, *Chem. Rev.* 2011, **112**, 1555-1614.
5 X. C. Wang, K. Maeda, A. Thomas, K. Takanabe, G. Xin, J. M. Carlsson, K. Domen and M. Antonietti, *Nat. Mater.* 2009, **8**, 76-80.
6 S. C. Yan, Z. S. Li and Z. G. Zou, *Langmuir* 2009, **25**, 10397-10401.
7 S. C. Yan, S. B. Lv, Z. S. Li and Z. G. Zou, *Dalton Trans.* 2010, **39**, 1488-1491.
8 Q. J. Xiang, J. G. Yu and M. Jaroniec, *J. Phys. Chem. C* 2011, **115**, 7355-7363.
9 (a) W. Ong, L. Tan, S. Chai, S. Yong and A. R. Mohamed, *Nanoscale*, 2014, **6**, 1946-2008; (b) X. Pan, M.Q. Yang, X. Fu, N. Zhang and Y.J. Xu, *Nanoscale*, 2013, **5**, 3601–3614; (c) Y. Wang, Q. Wang, X. Zhan, F. Wang, M. Safdarand and Jun He, *Nanoscale*, 2013, **5**, 8326–8339; (d) H. Yang, C. Sun, S. Qiao, J. Zou, G. Liu, S. C. Smith, H. Cheng and G. Q. Lu, *Nature* 2008, **453**, 638-641.
10 (a) H. Arakawa and K. Sayama, *Catal Surv Japan*, 2000, **4**, 75–80; (b) C. Richter,C. Jaye, E. Panaitescu, D. A. Fischer, L. H. Lewis, R. J. Willeya and L. Menon, *J. Mater. Chem.* 2009, **19**, 2963-2967; (c) X. Qiu, M. Miyauchi, H. Yu, H. Irie and K. Hashimoto, *J. Am. Chem. Soc.* 2010, **132**, 15259–15267
11 C. J. Pedersen, *J. Am. Chem. Soc.* 1967, **89**, 7017-7036.
12 Y. Li, F He, S Peng, D Gao, G Lu and S Li, *J. Mol. Catal. A: Chem* 2011, **341**, 71-76.
13 W.J. Hsieh, P.S. Shih, J.H. Lin, C.C. Lin, U.S. Chen, S.C. Huang, Y.S. Chang and H.C. Shih, *Thin Solid Films*, 2004, **469-470**, 120-126
14 R. E. Farsani, S. Raissi, A. Shokuhfar and A. Sedghi, *World Academy of Science, Eng. Technol.*, 2009, **20**, 430-433
15 K. Wu, T. Liu, C. Ma, B. Chang, R, Chen and X. Wang, *Environ. Sci. Pollut. Res.* 2014, **21**, 620–630
16 (a) J. R. Holst and E. G. Gillan, *J. Am. Chem. Soc.* 2008, **130**, 7373-7379; (b) K. Kailasam, J. D. Epping, A. Thomas, S. Losse and H. Junge, *Energy Environ. Sci.* 2011, **4**, 4668-4674; (c) J. Sun, J. Zhang, M. Zhang, M. Antonietti, X. Fu and X. Wang, *Nat. Comm.* 2012, **3**, 1.
17 S. J. Makowski, P. Kostler and W. Schnick, *Chem. Eur. J.* 2012, **18**, 3248-3257.
18 T. A. Luther, F. F. Stewart, J. L. Budzien, R.A. Laviolette, W. F. Bauer, M. K. Harrup, C. W. Allen and A. Elayan, *J. Phys. Chem. B* 2003, **107**, 3168-3176.
19 (a) B. V. Lotsch, M. Doblinger, J. Sehnert, L. Seyfarth, J. Senker, O. Oeckler and W. Schnick, *Chem. Eur. J.* 2007, **13**, 4969-4980; (b) B. Jürgens, E. Irran, J. Senker, P. Kroll, H. Müller and W. Schnick, *J. Am. Chem. Soc.* 2003, **125**, 10288-10300.
20 J. R. Lakowicz, *Principles of Fluorescence Spectroscopy*, 3rd ed.; Springer: Berlin, 2009.
21 M. Shalom, S. Inal, C. Fettkenhauer, D. Neher and M. Antonietti, *J. Am. Chem. Soc.* 2013, **135**, 7118-7121.
22 G. Xu, R. Funahashi, M. Shikano, I. Matsubara and Y. Zhou, *Appl. Phys. Lett.* 2002, **80**, 3760-3762.
23 S. C. Yan, Z. S. Li and Z. G. Zou, *Langmuir* 2010, **26**, 3894-3901